

# Cosmological and astrophysical bounds on a heavy sterile neutrino and the KARMEN anomaly

A.D. Dolgov<sup>1,2</sup>, S.H. Hansen<sup>3</sup>

*INFN section of Ferrara*

*Via del Paradiso 12, 44100 Ferrara, Italy*

G. Raffelt<sup>4</sup>

*Max-Planck-Institut für Physik (Werner-Heisenberg-Institut)*

*Föhringer Ring 6, 80805 München, Germany*

D.V. Semikoz<sup>5</sup>

*Max-Planck-Institut für Physik (Werner-Heisenberg-Institut)*

*Föhringer Ring 6, 80805 München, Germany*

*and*

*Institute of Nuclear Research of the Russian Academy of Sciences*

*60th October Anniversary Prospect 7a, Moscow 117312, Russia*

## Abstract

Constraints on the lifetime of the heavy sterile neutrino, that was proposed as a possible interpretation of the KARMEN anomaly, are derived from primordial nucleosynthesis and SN 1987A. Together with the recent experimental bounds on the  $\nu_s$  lifetime, SN 1987A completely excludes this interpretation. Nucleosynthesis arguments permit a narrow window for the lifetime in the interval 0.1–0.2 sec. If  $\nu_s$  possesses an anomalous interaction with nucleons, the SN bounds may not apply, while the nucleosynthesis ones would remain valid.

PACS: 14.60.St, 26.50.+x, 95.30.Cq

---

<sup>1</sup>Also: ITEP, Bol. Chermushkinskaya 25, Moscow 113259, Russia.

<sup>2</sup>e-mail: [dolgov@fe.infn.it](mailto:dolgov@fe.infn.it)

<sup>3</sup>e-mail: [sthansen@fe.infn.it](mailto:sthansen@fe.infn.it)

<sup>4</sup>e-mail: [raffelt@mppmu.mpg.de](mailto:raffelt@mppmu.mpg.de)

<sup>5</sup>e-mail: [semikoz@ms2.inr.ac.ru](mailto:semikoz@ms2.inr.ac.ru)

# 1 Introduction

In 1995 the KARMEN collaboration discovered an anomaly in the time distribution of the charged and neutral current events induced by neutrinos from  $\pi^+$  and  $\mu^+$  decays at rest [1]. This anomaly may be explained by the production of a new neutral particle in pion decay

$$\pi^+ \rightarrow \mu^+ + x^0 , \quad (1)$$

with the mass 33.9 MeV, barely permitted by the phase space, so that this particle moves with non-relativistic velocity. Its subsequent neutrino-producing decays could be the source of the delayed neutrinos observed in the experiment. The anomaly was recently confirmed by the same group [2] with better statistics and substantially reduced cosmic-ray background.

A search for  $x^0$  particles produced in the rare pion decay (1) was performed in 1995 by an experiment at PSI [3]. It gave an upper limit for the branching ratio of  $\text{BR}(\pi^+ \rightarrow \mu^+ + x^0) < 2.6 \times 10^{-8}$  at 95% CL.

Several candidates for  $x^0$  have been proposed in the literature. In ref. [4] the authors considered a sterile neutrino,  $x^0 \equiv \nu_s$ . Their conclusion was that the sterile-neutrino hypothesis is compatible with all laboratory constraints, but they noted possible problems with astrophysics and cosmology. Further laboratory constraints on this model were investigated in ref. [5], concluding that mixings of  $\nu_s$  with  $\nu_e$  and  $\nu_\mu$  must be very small, while a mixing with  $\nu_\tau$  was permitted. In this case  $\nu_s$  would predominantly decay through neutral-current interactions into  $\nu_\tau + \ell + \bar{\ell}$ , where  $\ell$  is any light lepton,  $\ell = \nu_e, \nu_\mu, \nu_\tau$ , or  $e^-$ . The lifetime of  $\nu_s$  with respect to this decay was estimated to be in the range

$$10^{-3} \text{ sec} < \tau_{\nu_s} < 150 \text{ sec} . \quad (2)$$

The lower bound on  $\tau_{\nu_s}$ , which comes from the experimental bound on the  $\nu_\tau$  mass (large mixing with  $\nu_s$  makes it too heavy), was discussed in ref. [6].

In ref. [7] it was suggested that  $x^0 \equiv \tilde{\chi}$  could be the lightest supersymmetric particle, photino or zino, that decayed through the channel

$$\tilde{\chi} \rightarrow \gamma + \nu_\mu . \quad (3)$$

The new data [2], however, do not agree with the predictions of the model so that recently a new version of supersymmetric model was considered [8], according to which the light neutralino decayed through a three body channel

$$\tilde{\chi} \rightarrow e^+ + e^- + \nu_{\mu,\tau} . \quad (4)$$

In the paper [9] a new decay mode of muons was proposed as a source of the anomaly:

$$\mu^+ \rightarrow e^+ + S , \quad (5)$$

where  $S$  is a scalar boson with mass 103.9 MeV. A search for these decays was reported in ref. [10] where the upper limit  $\text{BR}(\mu^+ \rightarrow e^+ + S) < 5.7 \times 10^{-4}$  was obtained. This limit, though it does not exclude the model, makes it more complicated.

Recent data by the NOMAD collaboration [11] permit to strengthen the bound on the mixing of  $\nu_s$  with  $\nu_\tau$ . Their expected lower limit on  $\tau_{\nu_s}$  is around 0.1 sec.

On the other hand, cosmology and astrophysics permit to obtain an upper bound on  $\tau_{\nu_s}$  that may be complementary to direct experiments. If this happens to be the case, then the explanation of the KARMEN anomaly by a 33.9 MeV sterile neutrino would be ruled out. Recently two papers have appeared [12, 13] where the observation of SN 1987A were used to put bounds on the properties of the proposed sterile neutrino or light neutralino. In the present paper we derive constraints on the lifetime of a 33.9 MeV sterile neutrino from both more detailed consideration of SN 1987A and of primordial nucleosynthesis. With the present-day accuracy of the data on the primordial light-element abundances, the bounds that are found from SN 1987A tend to be stronger than those found from primordial nucleosynthesis. However, the latter remain interesting, first, because they may be competitive in the nearest future with

an improved accuracy of the data on primordial nucleosynthesis, and second, in a hypothetical case where  $\nu_s$  would have an anomalously strong (stronger than the usual weak) interaction with nucleons. In that case the SN 1987A bounds would not apply, while the nucleosynthesis bounds would survive.

## 2 Primordial Nucleosynthesis

### 2.1 General Features

A heavy unstable sterile neutrino would influence big-bang nucleosynthesis (BBN) through its contribution to the cosmological energy density by speeding up the expansion and enlarging the frozen neutron-to-proton ratio,  $r_n = n/p$ , and less directly, though stronger, through its decay products,  $\nu_e$ ,  $\nu_\mu$ , and  $\nu_\tau$ . The impact of  $\nu_\mu$  and  $\nu_\tau$  on BBN is rather straightforward: their energy density increases with respect to the standard case and this also results in an increase of  $r_n$ . This effect can be described by the increased number of effective neutrino species  $N_\nu$  during BBN (in the standard case  $N_\nu = 3$ ). The increase of the energy density of  $\nu_e$ , due to decay of  $\nu_s$  into  $\nu_e$ , has an opposite effect on  $r_n$ . Though a larger energy density results in faster cooling, the increased number of  $\nu_e$  would preserve thermal equilibrium between neutrons and protons for a longer time and correspondingly the frozen  $n/p$ -ratio would become smaller. The second effect is stronger, so the net result is a smaller  $n/p$ -ratio. There is, however, another effect which is related to the distortion of the energy spectrum of  $\nu_e$  from the decays of  $\nu_s$ . If the spectrum is distorted at the high-energy tail, as is the case, then proton formation in the reaction  $n + \nu_e \rightarrow p + e^-$  would be less efficient than neutron creation in the reaction  $\bar{\nu}_e + p \rightarrow n + e^+$ . We found that this effect is quite significant. The decays of  $\nu_s$  into the  $e^+e^-$ -channel will inject more energy into the electromagnetic part of the primeval plasma and this will diminish the relative contribution of the energy density of light neutrinos and diminish  $r_n$ .

We could use the technique and numerical code from our earlier papers where the effects of non-equilibrium massless neutrinos (in the standard model) [14] and possibly

massive [15] and/or unstable [16] tau-neutrinos were precisely calculated. However, since we do not need the accuracy of a fraction of per cent achieved in these papers, we will use a simpler and considerably less time consuming approximate approach that we will now discuss.

## 2.2 The model

If the KARMEN anomaly is explained by a heavy sterile neutrino with  $m_{\nu_s} = 33.9$  MeV then, as was mentioned in the Introduction, it may only mix with  $\nu_\tau$ ,

$$\begin{aligned}\nu_\tau &= \nu_1 \cos \Theta + \nu_2 \sin \Theta , \\ \nu_s &= -\nu_1 \sin \Theta + \nu_2 \cos \Theta ,\end{aligned}\tag{6}$$

where  $\Theta$  is the vacuum mixing angle and  $\nu_1$  and  $\nu_2$  are the mass eigenstates; the mass difference is positive:  $\delta m^2 = m_2^2 - m_1^2 \approx (33.9 \text{ MeV})^2 > 0$ . Through neutral-current interactions  $\nu_s$  could decay into  $\nu_\tau$  and a pair of other light leptons. The corresponding processes and their matrix elements are presented in table 1. The lifetime of  $\nu_s$  is given by the expression

$$\tau_{\nu_s} \equiv \Gamma_{\nu_s}^{-1} = \left[ \frac{(1 + \tilde{g}_L^2 + g_R^2) G_F^2 m_{\nu_s}^5 (\sin^2 2\Theta)/4}{192\pi^3} \right]^{-1} \approx \frac{5.7 \times 10^{-4} \text{ sec}}{(\sin^2 2\Theta)/4} ,\tag{7}$$

where

$$\tilde{g}_L = -1/2 + \sin^2 \theta_W \text{ and } g_R = \sin^2 \theta_W .\tag{8}$$

According to the combined experimental data, the lifetime lies in the range

$$0.1 \text{ sec} < \tau_{\nu_s} < 150 \text{ sec}\tag{9}$$

and correspondingly

$$3.9 \times 10^{-3} < \sin 2\Theta < 0.15 .\tag{10}$$

Even with a very small mixing,  $\nu_s$  could be abundantly produced in the early universe when the temperature was higher than  $m_{\nu_s}$ . Their production rate can be estimated

as [17, 18]

$$\Gamma_{\nu_s} = \frac{1}{2} \sin^2 2\Theta_M \Gamma_W, \quad (11)$$

where  $\Gamma_W = 2.5 G_F^2 T^5$  is the averaged weak interaction rate and  $\Theta_M$  is the mixing angle in the medium. According to the calculations of refs. [17, 19]

$$\sin 2\Theta_M \approx \frac{(\sin 2\Theta)/2}{1 + 0.76 \times 10^{-19} T^6 (\delta m^2)^{-1}} \approx \frac{(\sin 2\Theta)/2}{1 + 6.6 \times 10^{-23} T^6}, \quad (12)$$

where  $T$  and  $\delta m^2$  are taken in MeV. One sees that matter effects are not important for  $T < 5$  GeV.

Comparing the production rate (11) with the Hubble expansion rate

$$H = \sqrt{\frac{8\pi^3}{90} g_*(T)} \frac{T^2}{M_{\text{Pl}}}, \quad (13)$$

we find that sterile neutrinos could be abundantly produced in the early universe if, roughly speaking,  $(\sin 2\Theta)^2 (T/3 \text{ MeV})^3 > 1$ . Even for  $\Theta$  at the lower limit given by the relation (10), the equilibrium condition is fulfilled for  $T \approx 120$  MeV. For this small value of  $\Theta$  the original equilibrium number density of  $\nu_s$  would be diluted at smaller  $T$  by annihilation of pions and muons. However, as we see in what follows, nucleosynthesis strongly disfavors large values of  $\tau_{\nu_s}$ . Correspondingly, for large mixing angles  $\nu_s$  remains in equilibrium for much smaller  $T$ , and this dilution is not essential.

The evolution of  $\nu_s$  at lower temperatures,  $T < m_{\nu_s}$ , is considered below. We calculate the number density of the heavy  $\nu_s$  assuming that initially they were in equilibrium and in the process of freeze-out they interacted with the thermal equilibrium bath of light particles. With the evident correction for the  $\nu_s$  decay, these calculations are very similar to the usual freeze-out calculation of massive species. There is one important difference however. Normally massive particles disappear in the process of mutual annihilation, so that the rate of freezing is proportional to the number density of the particle in question,  $\dot{n}_m/n_m \sim \sigma_{\text{ann}} n_m$ , which becomes exponentially small when  $T < m$ . Sterile neutrinos may also disappear in collisions with massless leptons

$$\nu_s + \ell_1 \rightarrow \ell_2 + \ell_3, \quad (14)$$

so their extinction through this process would be more efficient than by mutual annihilation,  $\nu_s + \bar{\nu}_s \rightarrow \text{all}$ . The decoupling temperature of the process (14) can be approximately found from the decoupling of the usual massless neutrinos at  $T_{\nu_\tau} \sim 2$  MeV by rescaling it by the mixing parameter,  $(\sin 2\Theta)^{2/3}$ . To obtain a better estimate we solve the corresponding kinetic equation for  $\nu_s$  in sec. 2.3. This permits us to determine the distribution function,  $f_{\nu_s}(x, y)$ , where

$$x = m_0 a(t) \quad \text{and} \quad y = p a(t) , \quad (15)$$

are convenient dimensionless variables with  $a(t)$  the cosmic scale factor and  $m_0$  the normalization mass that we choose as  $m_0 = 1$  MeV. In what follows we will often skip  $m_0$ , keeping in mind that the relevant quantities are measured in MeV. In terms of these variables, the kinetic equations have the form

$$(\partial_t - H p \partial_p) f = H x \partial_x f = I_{\text{coll}} , \quad (16)$$

where

$$\begin{aligned} I_{\text{coll}} = & \frac{1}{2E} \int \prod_i \left( \frac{d^3 p_i}{2E_i (2\pi)^3} \right) \prod_f \left( \frac{d^3 p_f}{2E_f (2\pi)^3} \right) \\ & \times (2\pi)^4 \delta^{(4)} \left( \sum_i p_i - \sum_f p_f \right) |A_{if}|^2 F(f_i, f_f) , \end{aligned} \quad (17)$$

is the collision integral and

$$F(f_i, f_f) = - \prod_i f_i \prod_f (1 - f_f) + \prod_f f_f \prod_i (1 - f_i) \quad (18)$$

with sub- $i$  and sub- $f$  meaning initial and final particles.

After the distribution function of  $\nu_s$  is found, the next step is to find the distribution functions of the light neutrinos and in particular their energy densities. The distributions of electrons and positrons are of course assumed to be very close to equilibrium because of their very fast thermalization due to the interaction with the photon bath. However, the evolution of the photon temperature, due to decay and

annihilation of the massive  $\nu_s$ , becomes different from the standard one,  $T_\gamma \sim 1/x$ , by an extra factor  $(1 + \Delta) > 1$ :

$$T_\gamma = [1 + \Delta(x)]/x . \quad (19)$$

At sufficiently high temperatures,  $T > T_W \sim 2$  MeV, light neutrinos and electrons/positrons were in strong contact, so that the neutrino distributions were also very close to the equilibrium ones. If  $\nu_s$  disappeared sufficiently early, while thermal equilibrium between  $e^\pm$  and neutrinos remained, then  $\nu_s$  would not have any observable effect on primordial abundances, because only the contribution of neutrino energy density relative to the energy density of  $e^\pm$  and  $\gamma$  is essential for nucleosynthesis. Hence a very short-lived  $\nu_s$  has a negligible impact on primordial abundances, while with an increasing lifetime the effect becomes stronger. Indeed at  $T < T_W$  the exchange of energy between neutrinos and electrons becomes very weak and the energy injected into the neutrino component is not immediately redistributed between all the particles. The branching ratio of the decay of  $\nu_s$  into  $e^+e^-$  is approximately 1/9, so that the neutrino component is heated much more than the electromagnetic one. As we mentioned above, this leads to a faster cooling and to a larger  $n/p$ -ratio.

So, for the numerical calculations we adopt the following procedure. We assume that at sufficiently high temperature, e.g.  $T_i = 5$  MeV, or equivalently at the initial value of the scale factor  $x_i = 1/T_i = 0.2$ , there is a complete thermal equilibrium between active neutrinos and electrons. Starting from that moment we calculate the corrections to the active neutrino distribution functions

$$\delta f_\nu = f_\nu - f_\nu^{\text{eq}} , \quad (20)$$

where the equilibrium distribution function is assumed to have the standard Fermi-Dirac form with a temperature that drops as  $1/x$ ,

$$f_\nu^{\text{eq}} = (e^y + 1)^{-1} . \quad (21)$$

The evolution of the photon temperature, i.e.  $\Delta(x)$ , is determined from the energy



balance equation

$$d\rho/dx = -3(\rho + p)/x , \quad (22)$$

where  $\rho$  and  $p$  are respectively the total energy and pressure densities in the cosmological plasma.

It is worth noting that we normalized the scale factor in such a way that at the initial moment  $x_i T_i = 1$ . If we change the initial moment for calculating  $\Delta$ , it would result in a different definition of  $x$ , but this is unobservable. We have checked that for  $x_i = 0.1-0.3$  the results weakly depend upon the value of  $x_i$ , and that the corrected neutrino distribution  $f_\nu = f_\nu^{\text{eq}} + \delta f$  quite accurately maintain the equilibrium shape with the same temperature as electrons,  $T_\nu = T_\gamma$  at these early times.

We made several assumptions that permitted to simplify calculations very much:  $\nu_s$  was assumed non-relativistic, the equilibrium distribution functions “inside” the collision integral were taken in the Boltzmann approximation, while “outside” they were taken in Fermi-Dirac form, and the kinetic equations for  $\delta f_\nu$  were taken in a simplified form, so that some fraction of neutrino energy was lost (see sec. 2.4). All these assumptions lead to a weaker impact of  $\nu_s$  on nucleosynthesis, so the real bound should be somewhat stronger than what is presented below.

One more comment is in order. We do not take into account oscillations between  $\nu_s$  and  $\nu_\tau$  for  $T < m_{\nu_s}$ . This is perfectly justified because in the interesting range of neutrino energies the oscillation frequency is so high and the velocities of  $\nu_s$  and  $\nu_\tau$  are so much different that the coherence is quickly lost and they can be considered as independent particles. Medium effects are also not important for the considered positive mass difference  $\delta m^2 \approx 10^3 \text{ MeV}^2$ .

### 2.3 Evolution of Heavy Neutrinos

The evolution of the occupation number of  $\nu_s$  is determined by its decays and inverse decays, listed in table 1, and by the reactions (14) with all possible sets of light leptons permitted by quantum numbers, presented in table 2. Taking both contributions into

the collision integral and assuming that the massless species are in thermal equilibrium with temperature  $T$  and that both helicity states of  $\nu_s$  are equally populated, we obtain

$$\partial_x f_{\nu_s}(x, y) = \frac{1.48 x}{\tau_{\nu_s}(\text{sec})} \left( \frac{10.75}{g_*(T)} \right)^{1/2} \frac{f_{\nu_s}^{\text{eq}} - f_{\nu_s}}{(Tx)^2} \left[ \frac{m_{\nu_s}}{E_{\nu_s}} + \frac{3 \times 2^7 T^3}{m_{\nu_s}^3} \left( \frac{3\zeta(3)}{4} + \frac{7\pi^4}{144} \left( \frac{E_{\nu_s} T}{m_{\nu_s}^2} + \frac{p_{\nu_s}^2 T}{3E_{\nu_s} m_{\nu_s}^2} \right) \right) \right], \quad (23)$$

where  $E_{\nu_s} = \sqrt{m_{\nu_s}^2 + (y/x)^2}$  and  $p_{\nu_s} = y/x$  are the energy and momentum of  $\nu_s$  respectively and  $g_*(T)$  is the effective number of massless species in the plasma determined as the ratio of the total energy density to the equilibrium energy density of one bosonic species with temperature  $T$ ,  $g_* = \rho_{\text{tot}}/(\pi^2 T^4/30)$ . The coefficient 1.48 comes from expressing the lifetime in sec according to the relation  $1/\text{MeV} = 0.658 \times 10^{-21}$  sec and from the value of the Hubble parameter  $H = \sqrt{8\pi\rho_{\text{tot}}/3M_{\text{Pl}}^2}$ . The first term in square brackets,  $m_{\nu_s}/E_{\nu_s}$ , comes from summing the squared matrix elements in table 1 (decay) while the rest is obtained by using that the sum of the squared matrix elements from table 2 (collisions) can be written as

$$|M|^2 \sim \left( 1 + \tilde{g}_L^2 + g_R^2 \right) [(p_1 \cdot p_2)(p_3 \cdot p_4) + 2(p_1 \cdot p_4)(p_3 \cdot p_2)]. \quad (24)$$

The assumption of Boltzmann statistics for massless leptons considerably simplifies the calculations, because the integral over their momenta can be taken explicitly. This approximation results in a larger value of the collision integral, i.e. in faster decay and reaction rates and correspondingly to a smaller abundance of  $\nu_s$ . Thus the restriction on  $\tau_{\nu_s}$  obtained in this approximation is weaker than the real one.

At high temperatures,  $T > 5$  MeV, (23) was integrated with the simplifying assumption  $Tx = 1$ . This also leads to a weaker bound on  $\tau_{\nu_s}$ . Assuming entropy conservation one can check that  $Tx$  may change by a factor 1.1 due to  $\nu_s$  decays and annihilation. In fact the effect is stronger because the number density of  $\nu_s$  is much larger than the equilibrium one. However, since we started at  $T = 5$  MeV  $< m_{\nu_s}$ , when the energy density of  $\nu_{\nu_s}$  was already somewhat suppressed, the variation of  $Tx$  from that moment would be weaker.

Naively one would expect a variation of  $f_{\nu_s}$  similar to the variation of  $Tx$ . However, it is argued below that the effect may be much stronger. Indeed, since  $\nu_s$  disappears in the collisions with massless particles, its number density is much more sensitive to the variation of the coefficient in front of the collision integral. In the case of the standard freezing in two-body annihilation the frozen number density,  $n_f$ , is known to be inversely proportional to the annihilation cross-section. This is not true for the case of reactions (14). One can solve the kinetic equation explicitly and check that the result is exponentially sensitive to the coefficient in front of  $(f_{\nu_s}^{\text{eq}} - f_{\nu_s})$ . Therefore we took the variation of  $Tx$  into account, starting from  $x_i = 0.2$ , according to the energy balance law (22), see also (34). A simpler and more common method based on entropy conservation is not accurate enough because the sterile neutrinos strongly deviate from equilibrium in the essential range of temperatures and thus entropy is not conserved.

In the non-relativistic limit we may integrate both sides of (23) over  $d^3y/(2\pi)^3$  to obtain the number density of  $\nu_s$  in the comoving volume

$$\bar{n}_{\nu_s} = x^3 n_{\nu_s} = \bar{n}_{\nu_s}^{\text{eq}} - \int_0^x dx_1 \frac{d\bar{n}_{\nu_s}^{\text{eq}}}{dx_1} \exp \left[ \int_{x_1}^x dx_2 B(x_2) \right], \quad (25)$$

where

$$B(x) = \frac{1.48x}{(Tx)^2(\tau_{\nu_s}/\text{sec})} \left( \frac{10.75}{g_*(T)} \right)^{1/2} \left[ 1 + \frac{3 \times 2^7 (Tx)^3}{x^3 m_{\nu_s}^3} \left( \frac{3\zeta(3)}{4} + \frac{7\pi^4}{144} (Tx) \right) \right]. \quad (26)$$

Usually  $Tx$  is assumed to be constant, quite often normalized as  $Tx = 1$ . A small variation of this quantity usually is not very important for the value of  $\bar{n}$ . In our case, however, estimating the integral by the saddle point method reveals that the dependence on  $Tx$  appears in the exponent and the effect may be significant even for a small variation of  $Tx$ . The dependence on  $Tx$  for the scattering term results in an increase of  $\bar{n}_{\nu_s}$ , while that for the decay term results in a decrease of  $\bar{n}_{\nu_s}$ .

The results of the numerical solution of (23) for different values of lifetimes are presented in figs. 1, 2, and 3. The first one shows the evolution of  $x^3 n_{\nu_s}$  for  $\tau_{\nu_s} = 0.1, 0.2,$  and  $0.3$ , the second is  $x^4 \rho_{\nu_s}$ , while the third figure is a snap-shot of the

distribution functions,  $f_{\nu_s}$ , at  $x = 1$ . All the distributions are significantly higher than the equilibrium ones. For example, the equilibrium distribution is about 10 orders of magnitude below the calculated curve for  $\tau_{\nu_s} = 0.1$ .

## 2.4 Light Neutrinos

At the onset of nucleosynthesis,  $\nu_s$  practically disappeared from the primeval plasma, at least for sufficiently small lifetimes, which are near the bound obtained below. However, the products of their decays and annihilation distorted the standard nucleosynthesis conditions: the energy density as well as the spectrum of neutrinos were different from the standard ones, and this changed the light element abundances.

We will look for the solution of the kinetic equations governing the evolution of the distribution functions of light neutrinos in the form

$$f_{\nu_a}(x, y) = (1 + e^y)^{-1} + \delta f_{\nu_a}(x, y) , \quad (27)$$

where  $a = e, \mu, \text{ or } \tau$ . The first term is equal to the equilibrium distribution function for the case when the temperature drops as the inverse scale factor, i.e.  $Tx = 1$ . In reality this is not the case and the function  $\delta f$  takes into account both the variation of  $Tx$  and the spectrum modification of the active neutrinos.

The distribution of  $e^\pm$  always has the equilibrium form,  $f_e = [1 + \exp(E/T)]^{-1} = [1 + \exp(y/Tx)]^{-1}$  and the product  $Tx$  is taken in the form

$$Tx = 1 + \Delta(x) , \quad (28)$$

where  $\Delta$  is assumed to be small, such that a perturbative expansion in  $\Delta$  can be made. A similar first-order perturbative expansion is made with respect to  $\delta f$ , so that the collision integral becomes linear in terms of  $\Delta$  and  $\delta f$ .

It is assumed that initially both  $\delta f$  and  $\Delta$  were zero. To this end one should find an appropriate value of the initial “time”,  $x_i$ , or temperature,  $T_i$ . The temperature should be sufficiently small, such that the number density of  $\nu_s$  is already low and hence the function  $\Delta$  would not rise too much. On the other hand, the temperature

should not be too low, otherwise equilibrium between neutrinos and electrons would not be established and the assumption of  $\delta f = 0$  could be grossly wrong. As we see in what follows, convenient initial values that satisfy both conditions are  $x_i \sim 0.2$  and  $T_i \sim 5$  MeV for  $\tau_{\nu_s} \sim 0.2$  sec. Of course, the later rise of temperature by the well known factor 1.4 because of  $e^+e^-$ -annihilation is taken into account explicitly.

## 2.5 Collision Integral and Source Term

There are two kinds of terms in the collision integral, “easy” ones where the unknown function  $\delta f$  depends upon the external variable  $y$ , which is not integrated upon, and “difficult” ones when  $\delta f$  is under the integral. The terms of the first kind come, with negative sign, from external particles in the initial state. They give

$$\partial_x \delta f_{\nu_e}(x, y) = -0.26 \left( \frac{10.75}{g_*} \right)^{1/2} \delta f_{\nu_e} (1 + g_L^2 + g_R^2)(y/x^4), \quad (29)$$

where  $g_L = \sin^2 \theta_W + 0.5$ , while  $g_R = \sin^2 \theta_W$ . For  $\nu_\mu$  and  $\nu_\tau$  the functions  $\tilde{g}_L$  and  $g_R$  are given by expressions (8). Using the simple expression (29) one finds that the rate of approach of  $\nu_e$  to equilibrium is given by

$$\delta f_{\nu_e} \sim \exp(-0.13 y/x^3). \quad (30)$$

One sees that equilibrium would be efficiently restored for  $\nu_e$  if  $x < 0.5 y^{1/3}$  or  $T > 2y^{-1/3}$  MeV, while for  $\nu_{\mu,\tau}$  equilibrium would be restored if  $T > 2.25 y^{-1/3}$  MeV. These results are close to the standard estimates known in the literature (for the most recent ones see e.g. [20]). However, there are the following drawbacks in this derivation. First, it was done under the assumption that the source of distortion acted for a finite time and thus (30) could be valid only after the source has been switched off. If there is a constantly working source,  $S(x, y)$ , equilibrium is always distorted roughly by the factor  $S/\Gamma$ , where  $\Gamma$  is the effective reaction rate. Another and more serious argument against the validity of (30) is that the “difficult” part of the collision integral was neglected. One can see from the general expressions (17,18) that  $\delta f$  also appears under the integral over momenta, and it can be seen that it comes mostly with

a positive sign. These terms counteract the smoothing action of expression (29) and shift equilibrium restoration to considerably higher temperatures. One can take them into account exactly, numerically solving the kinetic equations with the exact collision integral that can be reduced down to a 2-dimensional integration over particle energies (see e.g. [14]), but this is a very time consuming procedure. Instead we will here use a much simpler approach. We will approximately represent such “difficult” terms by the integrals over energy chosen in such a way that the kinetic equations satisfy the law of particle conservation in the comoving volume if only elastic scattering is taken into account, i.e. the kinetic equation should automatically give  $\partial_x(x^3 n) = 0$ . The exact equations should simultaneously satisfy energy conservation law, but working with the exact equations is much more complicated. We checked the validity of our approximate procedure for a case of a more simple reaction amplitude, where we compared the approximate and exact results and found very good agreement. The approximation that we use breaks the energy conservation law in the kinetic equation, so that some small fraction of energy going into light particles from  $\nu_s$  decays and/or annihilation is lost. This diminishes the effects that we are discussing so that the real constraints on  $\tau_{\nu_s}$  should be stronger.

The kinetic equations for light neutrinos in this approximation can be written as

$$\begin{aligned} \partial_x \delta f_{\nu_e}(x, y) = & S_{\nu_e}(x, y) + 0.26 \left( \frac{10.75}{g_*} \right)^{1/2} (1 + g_L^2 + g_R^2)(y/x^4) \\ & \times \left\{ -\delta f_{\nu_e} + \frac{2}{15} \frac{e^{-y}}{1 + g_L^2 + g_R^2} [1 + 0.75(g_L^2 + g_R^2)] \right. \\ & \times \left[ \int dy_2 y_2^3 \delta f_{\nu_e}(x, y_2) + \frac{1}{8} \int dy_2 y_2^3 (\delta f_{\nu_\mu}(x, y_2) + \delta f_{\nu_\tau}(x, y_2)) \right] \\ & \left. + \frac{3}{5} \Delta(x) \frac{g_L^2 + g_R^2}{1 + g_L^2 + g_R^2} e^{-y} (11y/12 - 1) \right\}. \end{aligned} \quad (31)$$

The coefficients  $g_{L,R}$  for  $\nu_{\mu,\tau}$  are given by (8) and for  $\nu_e$  are presented after (29). The source term  $S$  describes injection of non-equilibrium neutrinos by  $\nu_s$  decays or reactions (14) with light leptons. In what follows we include only decays. We have estimated the contributions of the reactions (14) and found that they slightly improve

the restrictions that we have obtained. For  $\nu_e$ ,  $\nu_\mu$ , and  $\nu_\tau$  the contributions of the decay term are respectively

$$\begin{aligned}
S_{\nu_e, \nu_\mu}(x, y) &= \frac{0.012}{\tau_{\nu_s} x^2} \left( \frac{10.75}{g_*} \right)^{1/2} \left( 1 - \frac{16y}{9m_{\nu_s} x} \right) (n_{\nu_s} - n_{\nu_s}^{\text{eq}}) \theta(m_{\nu_s} x/2 - y) , \quad (32) \\
S_{\nu_\tau}(x, y) &= \frac{0.024}{\tau_{\nu_s} x^2} \left( \frac{10.75}{g_*} \right)^{1/2} \left[ 1 - \frac{16y}{9m_{\nu_s} x} + \frac{2}{3} (1 + \tilde{g}_L^2 + g_R^2) \left( 1 - \frac{4y}{3m_{\nu_s} x} \right) \right] \\
&\quad \times (n_{\nu_s} - n_{\nu_s}^{\text{eq}}) \theta(m_{\nu_s} x/2 - y) , \quad (33)
\end{aligned}$$

where  $n_{\nu_s}(x)$  is the number density of  $\nu_s$  and  $\theta(y)$  is the step function which ensures energy conservation in the decay. The factor 0.012 comes from the product of the branching ratio  $\text{BR} = 96/4/(1 + \tilde{g}_L^2 + g_R^2) = 21.3$  with the factors  $3/m_{\nu_s}^3 = 7.7 \times 10^{-5}$  ( $m_{\nu_s}$  in MeV) from the normalization, we divide by  $2/\pi^2 = 0.203$  from the number density, and 6.582 from the relation between MeV and sec. Dividing by the Hubble parameter gives a factor,  $1.221/(1.88\sqrt{8\pi/3}) = 0.2244$ , and we find  $21.3 \times (7.7 \times 10^{-5}) \times 0.2244 \times 6.582/0.203 = 0.012$ .

The coefficient in front of the collision integral is in reality momentum dependent, and hence is slightly different from 0.4 for  $\nu_e$  (and 0.29 for  $\nu_{\mu, \tau}$ ), which are often used in the literature. We extracted the correct momentum dependent coefficients from our Standard Model code [14], and used this in the calculations. This slightly weakens the bound on the lifetime.

The function  $\Delta(x)$  is determined from the energy balance condition (22) which in the present case reads

$$\frac{d\Delta}{dx} = -\frac{1}{4x^4 \rho_{EM}} \left[ \frac{xd(x^3 \rho_{\nu_s})}{dx} + \frac{d(x^4 \delta \rho_\nu)}{dx} \right] , \quad (34)$$

where  $\rho_{EM}$  is the energy density in the electromagnetic sector, and  $\rho_{\nu_s}$  and  $\rho_\nu$  are the energy density of  $\nu_s$  and the total energy density of all light neutrinos respectively. We also used another method for calculating  $Tx$  starting from earlier times and obtained stronger results, so we believe that the limits that we obtain here are quite safe.

## 2.6 A Few Numerical Technicalities

Let us summarize a few technicalities related to the numerical approach. We divide the time into 3 regions. First we integrate only (23) from very high temperatures,  $T = 50$  MeV ( $x = 0.02$ ) and until  $T = 5$  MeV ( $x = 0.2$ ). We assume that initially the sterile particles are in equilibrium (see sec. 2.2). In this way we can follow the freeze out and initial decay of the sterile particles, without worrying about the equilibrium active neutrinos and the electromagnetic plasma. In the next region,  $0.2 < x < 50$ , we solve (23, 32, 34) with the initial values  $\Delta = 0$  and  $\delta f_{\nu_{\text{active}}} = 0$ . It is worth mentioning that from the very beginning we separately calculate and include the annihilation of the electrons, which increase the photon temperature with a standard factor 1.4. Finally, for very high  $x > 50$  ( $T < 0.03$  MeV) when all sterile neutrinos have disappeared and the active neutrinos have long decoupled, we solved only the kinetic equations governing the  $n$ - $p$ -reactions needed for the nucleosynthesis code. We use an 800 point grid in momentum in the region  $0 < y < 80$ , and checked that the results are insensitive to the doubling of the grid. For the BBN calculations we use  $\eta_{10} = 5$ .

## 2.7 Results

We have solved (23, 32, 34) numerically for different lifetimes. In fig. 1 we plot the evolution of the normalized number density,  $x^3 n_{\nu_s}$ , as a function of  $x$ . One sees for  $\tau_{\nu_s} = 0.3$  how  $\nu_s$  first freeze out, followed by the subsequent decay. In fig. 2 a similar plot of the normalized energy density,  $x^4 \rho_{\nu_s}$ , is presented as a function of  $x$ , and the effect of the sterile particle being massive is evident. In fig. 3 we present a snap-shot of the distribution function at the time  $x = 1$ . The equilibrium distribution function at this time is about 10 orders of magnitude smaller than the curve for  $\tau = 0.1$  sec.

The calculated energy densities of all light neutrino species relative to the electromagnetic energy density,  $\rho_e + \rho_\gamma$ , are presented in fig. 4 as functions of  $x$ . One sees that this fraction is higher for longer lifetimes, especially around the time  $x = 1$ ,



when the  $n/p$ -ratio freezes out, leading to an expected increase in the final helium abundance. In fig. 5 a snap-shot of the spectrum of  $\nu_e$ , namely  $y^2 f_{\nu_e}$  and the distortion  $y^2 \delta f_{\nu_e}$  are presented for  $x = 1$  for the lifetimes 0.1, 0.2, 0.3. A distortion of the electronic neutrino spectrum has a strong impact on nucleosynthesis, while  $\nu_\mu$  and  $\nu_\tau$  act only by their total energy density. It is noteworthy that the increase in  $\rho_{\nu_e}$  acts in the opposite direction to an increase in  $\rho_{\nu_\mu, \nu_\tau}$ , since it reduces the effective number of light neutrinos, or in other words, it gives rise to a smaller mass fraction of primordial  ${}^4\text{He}$ , while an increase in the high energy part of  $\nu_e$  spectrum results in a larger mass fraction of  ${}^4\text{He}$ .

The results of the calculations have been imported into the modified Kawano [21] nucleosynthesis code, and the abundances of all light elements have been calculated. At each time step  $x$ , we find the corresponding photon temperature and total energy density. Furthermore we integrate the kinetic equation governing the  $n/p$  evolution taking into account the distorted spectrum of  $\nu_e$ . The final helium abundance is presented as a function of the  $\nu_s$  lifetime in fig. 6. By translating these results into effective number of neutrinos one sees that if we allow for  $\Delta N = 0.2$  (as suggested by [22]), then only lifetimes lower than  $\tau_{\nu_s} = 0.17$  sec are permitted. If one is more conservative and allows for one extra neutrino species,  $\Delta N = 1.0$ , then lifetimes longer than  $\tau_{\nu_s} = 0.24$  sec are excluded. A drop in the helium abundance around  $\tau_{\nu_s} = 0.1$  is related to the dominant role of the  $\nu_e$  energy density, since the spectrum distortion is shifted to smaller energies.

Finally in fig. 7 we compare the KARMEN experimental data with the bound obtained from BBN. One sees that the expected new data from the NOMAD Collaboration together with our BBN bound leave a small allowed window for a sterile neutrino with a lifetime around 0.1–0.2 sec.

### 3 Supernova Limits

### 3.1 Small Mixing Angle

The mixing angles of sterile neutrinos with the standard active flavors is tightly constrained by standard arguments related to supernova (SN) physics and to the neutrino observations of SN 1987A. Some of these arguments have been sketched out in the context of the KARMEN anomaly in Ref. [4].

The simplest limit arises from the “energy-loss argument.” The SN 1987A observations imply that a SN core may not emit too much energy in an “invisible channel” as this would unduly shorten the observed neutrino burst. Reasonably accurate limits are obtained by demanding that the “exotic” energy-loss rate should obey [23, 24]

$$\epsilon \lesssim 10^{19} \text{ erg g}^{-1} \text{ s}^{-1} , \quad (35)$$

where  $\epsilon$  is to be calculated at typical average conditions of a SN core ( $\rho = 3 \times 10^{14} \text{ g cm}^{-3}$ ,  $T = 30 \text{ MeV}$ ).

Sterile neutrinos  $\nu_s$  are produced because they mix with one of the standard ones. If the standard neutrino masses are all in the sub-eV range, the assumed sterile neutrino mass of  $m_{\nu_s} = 33.9 \text{ MeV}$  assures a mass difference so large that medium effects on the oscillations can be neglected. The oscillation frequency is so large that a standard neutrino  $\nu_a$ , once produced, oscillates many times before collisions interrupt the coherent development of the flavor amplitude. The average probability of finding the original  $\nu_a$  in the  $\nu_s$  flavor state is  $\frac{1}{2} \sin^2(2\Theta)$  where  $\Theta$  is the  $\nu_a$ - $\nu_s$ -mixing angle. Oscillations are interrupted with the collision rate  $\Gamma$  of the  $\nu_a$  flavor, leading to the standard sterile-neutrino production rate of  $\frac{1}{2} \sin^2(2\Theta)\Gamma$ .

We estimate  $\Gamma$  as the neutral-current collision rate on free nucleons, ignoring correlation and degeneracy effects, so that:

$$\Gamma = \frac{C_V^2 + 3C_A^2}{\pi} G_F^2 n_B E_\nu^2 , \quad (36)$$

with  $G_F$  the Fermi constant and  $n_B$  the number density of baryons (nucleons). For a mix of protons and neutrons we use an average neutral-current coupling constant of

$(C_V^2 + 3C_A^2) \approx 1$ . If we further assume that the trapped active neutrinos do not have a significant chemical potential (true for  $\nu_\mu$  and  $\nu_\tau$ , but not for  $\nu_e$ ), the energy-loss rate is

$$\epsilon_{\nu_s} = \frac{\sin^2(2\Theta)}{2} \frac{G_F^2}{\pi^3 m_N} \int_0^\infty dE_\nu \frac{E_\nu^5}{e^{E_\nu/T} + 1}, \quad (37)$$

where  $m_N$  is the nucleon mass. For simplicity we use Maxwell-Boltzmann statistics for the neutrinos (we ignore the +1 in the denominator under the integral) and find:

$$\begin{aligned} \epsilon_{\nu_s} &= \frac{\sin^2(2\Theta)}{2} \frac{120 G_F^2 T^6}{\pi^3 m_N}, \\ &= \sin^2(2\Theta) 2.8 \times 10^{26} \text{ erg g}^{-1} \text{ s}^{-1} T_{30}^6 \end{aligned} \quad (38)$$

where  $T_{30} = T/30$  MeV. Comparing this result with (35) leads to a limit

$$\sin^2(2\Theta) \lesssim 3 \times 10^{-8} T_{30}^{-6}. \quad (39)$$

The temperature  $T = 30$  MeV is at the lower end of what is found in typical numerical calculations so that this limit is reasonably conservative.

For the mixing with  $\nu_e$  the limit is more restrictive because the electron neutrinos in a SN core are highly degenerate, leading to a larger conversion rate and a larger amount of energy liberated per collision. Several authors found  $\sin^2(2\Theta) \lesssim 10^{-10}$  for this case [25, 26].

In our calculation of the emission rate we have taken the  $\nu_s$  to be effectively massless. The average energy of trapped standard neutrinos is about  $3T$  which far exceeds  $m_{\nu_s}$ . The scattering cross section scales with  $E_\nu^2$ , favoring the emission of high-energy neutrinos. The average  $\nu_s$  energy emerging from a SN core is thus found to be about  $5T$  so that neglecting  $m_{\nu_s}$  is a good approximation—the  $\nu_s$  are highly relativistic.

The KARMEN experiment implies that the lifetime of  $\nu_s$  exceeds about 0.1 s so that these particles escape from the SN before decaying. On the other hand, they must decay on the long way from SN 1987A to us. If the decay products include

$e^+e^-$  pairs one will also get  $\gamma$  rays from inner bremsstrahlung in the decay. The non-observation of a  $\gamma$  ray burst coinciding with SN 1987A then leads to further limits [23, 24].

The decay products likely would include standard neutrinos which would have shown up in the detectors. However, because of the high energies of the sterile neutrinos which are representative of the SN core temperature, such events would have much larger energies than those expected from thermal neutrino emission at the neutrino sphere. Therefore, the emission of sterile neutrinos from the core and their subsequent decay cannot mimic the standard SN neutrino signal.

### 3.2 Large Mixing Angle

These upper limits on the mixing angle are only valid if the sterile neutrinos actually escape from the SN core after production, a condition that is not satisfied if one of the mixing angles is too large. Since the mixing angle between  $\nu_e$  or  $\nu_\mu$  and  $\nu_s$  is already constrained from laboratory experiments to be small in this sense, we worry here only about the  $\nu_\tau$ - $\nu_s$  mixing angle. We continue to assume that the standard-neutrino mass eigenstates are small so that the mass difference and hence the oscillation frequency between  $\nu_\tau$  and  $\nu_s$  will be large compared to a typical collision rate in a SN core and that the mixing angle in the medium is identical to the vacuum mixing angle. Therefore, after production the chance of finding a  $\nu_s$  in the active  $\nu_\tau$  state will be given by the average value  $\frac{1}{2} \sin^2(2\Theta)$ . If the mixing angle is large this will mean that the sterile neutrino essentially acts as an active one. It will be trapped, and the energy-loss argument is not applicable.

If the mixing angle is not quite maximal, sterile neutrinos will still be trapped, but their mean free path will be larger than that of an active flavor. Energy is transported out of a SN core by neutrino diffusion, a mechanism which is more effective if the mfp is larger. Simply put, a neutrino can transport energy over distances of order the mfp so that more distant regions are thermally coupled if the mfp becomes larger. Most of

the transporting of energy is done by the most weakly coupled particles which are still trapped. For example, in a SN core the photon contribution to the energy transport is negligible because their mfp is very much smaller than that of standard neutrinos. Conversely, the contribution of sterile neutrinos will *increase* with an increasing mfp, i.e. with a decreasing  $\sin^2(2\Theta)$ .

The effect on the SN 1987A signal will be identical to the effect of freely escaping sterile neutrinos, i.e. the signal will be shortened. We stress that the signal duration is determined by the diffusion time scale throughout the star. Therefore, increasing the mfp in the deep interior of the star shortens the cooling time scale. In a numerical study [27] the neutrino opacities were artificially decreased. It was found that the efficiency of neutrino transfer in the star should not be more than about twice the standard value to remain consistent with the SN 1987A signal characteristics. Likewise, in a different study [28] the number of standard neutrino flavors was artificially increased, again leading to an increased efficiency of energy transfer. Doubling the effective number of neutrino flavors appears excluded from the SN 1987A data.

The interaction rate of sterile neutrinos is that of a standard  $\nu_\tau$ , times  $\frac{1}{2} \sin^2(2\Theta)$ . Conversely, the collision rate for  $\nu_\tau$  is  $1 - \frac{1}{2} \sin^2(2\Theta)$  times the standard rate because a  $\nu_\tau$  has an average chance  $1 - \frac{1}{2} \sin^2(2\Theta)$  of being measured as a  $\nu_s$ . Assuming that the standard transfer of energy is dominated by  $\nu_\mu$ ,  $\nu_\tau$  and their anti-particles (the mfp for  $\nu_e$  and  $\bar{\nu}_e$  is much shorter due to charged-current reactions), then adding the sterile neutrino will enhance the rate of energy transfer by a factor

$$\frac{1}{1+1} \left( 1 + \frac{1}{1 - \frac{1}{2} \sin^2(2\Theta)} + \frac{1}{\frac{1}{2} \sin^2(2\Theta)} \right). \quad (40)$$

Maximal mixing corresponds to  $\sin^2(2\Theta) = 1$ , implying that both  $\nu_\tau$  and  $\nu_s$  each scatter with half the standard rate, so their mfp is each increased by a factor of 2. Moreover, the sterile neutrino contributes a second channel for the transfer of energy. Therefore, the energy flux carried by maximally mixed  $\nu_s$  and  $\nu_\tau$  is four times that carried by a standard  $\nu_\tau$ . This explains the limiting behavior of (40) for maximal mixing.

The new experimental limit on the  $\nu_s$ - $\nu_\tau$  mixing angle is  $\sin^2(2\Theta) < 10^{-2}$ . Therefore, the efficiency of energy transfer out of a SN core would be enhanced by more than two orders of magnitude. Such an enhancement is certainly not compatible with the SN 1987A signal, implying that the mixing angle has to be very small, i.e. that it must obey (39). Therefore, the loop hole of a large  $\nu_s$ - $\nu_\tau$  mixing angle has been plugged by the new experimental constraints.

## 4 Conclusion

Cosmological and astrophysical arguments seem to exclude the interpretation of the KARMEN anomaly by an unstable sterile neutrino mixed with  $\nu_\tau$ . The arguments based on SN 1987A are stronger than the nucleosynthesis bound. The supernova limit is given by (39), i.e.  $\tau_{\nu_s} > 6 \times 10^4$  sec. This result, together with the direct experimental constraints on  $\nu_\tau$ , completely excludes a 33.9 MeV sterile neutrino. Primordial nucleosynthesis permits to exclude roughly  $\tau_{\nu_s} > 0.2$  sec. So with the existing direct experimental limits, some window,  $\tau_{\nu_s} = 0.1 - 0.2$  sec, remains open. The simplifications that we made in deriving the BBN bound typically lead to a weaker result, so the real bound may be somewhat stronger. However, if exact calculations confirm the decrease of  ${}^4\text{He}$  around  $\tau_{\nu_s} = 0.1$  found in this paper, then BBN will never exclude lifetimes  $\sim 0.1$  sec.

The effect happens to be surprisingly sensitive to usually neglected phenomena, particularly the shape of the  $\nu_e$  spectrum and to the non-adiabatic variation of temperature. We hope to do exact (but rather long) calculations later. Together with a possible improvement of the observational data on light element abundances and a better understanding of the subsequent changes of light elements in the course of cosmological evolution, the BBN bound may become competitive with the supernova one. If so, the very attractive hypothesis of a 33.9 MeV sterile  $\nu_s$  would be killed by two independent arguments. Moreover, one may imagine a case when the supernova arguments are not applicable, while the nucleosynthesis ones still operate. For exam-

ple, if  $\nu_s$  possesses an anomalously strong interaction with nucleons (stronger than the usual weak one), then it would not noticeably change the energetics of supernovae that we described here, but would affect nucleosynthesis practically at the same level as discussed in section 2. This new interaction might be related to the anomalously high mass of  $\nu_s$ . If this is the case then a small window for a 33.9 MeV  $\nu_s$  with lifetime  $\tau_{\nu_s} = 0.1\text{--}0.2$  sec, still exists at the present time, and stronger experimental bounds, as well as more accurate calculations of the impact of  $\nu_s$  on primordial nucleosynthesis, are needed.

## Acknowledgment

We are grateful to N. Krasnikov who brought this subject to our attention. In Munich, this work was partly supported by the Deutsche Forschungsgemeinschaft under grant No. SFB 375. DS thanks the NOMAD collaboration, in particular L. DiLella, L. Camilleri, S. Gninenko and A. Kovzelev, for the invitation and hospitality during their December-1999 collaboration meeting where this work was presented.

Process	S	$2^{-5}G_F^{-2} U_{s\tau} ^{-2}S A ^2$
$\nu_s \rightarrow \nu_\tau + \nu_\tau + \bar{\nu}_\tau$	1/2	$2(p_1 \cdot p_4)(p_2 \cdot p_3)$
$\nu_s \rightarrow \nu_\tau + \nu_{e(\mu)} + \bar{\nu}_{e(\mu)}$	1	$(p_1 \cdot p_4)(p_2 \cdot p_3)$
$\nu_s \rightarrow \nu_\tau + e^+ + e^-$	1	$4[(\tilde{g}_L^2(p_1 \cdot p_4)(p_2 \cdot p_3) + g_R^2(p_1 \cdot p_3)(p_2 \cdot p_4) + \tilde{g}_L g_R m_e^2(p_1 \cdot p_2))]$

**Table 1:** Matrix elements for decay processes;  $\tilde{g}_L = g_L - 1 = -\frac{1}{2} + \sin^2 \theta_W$  and  $g_R = \sin^2 \theta_W$ .

Process	S	$2^{-5}G_F^{-2} U_{s\tau} ^{-2}S A ^2$
$\nu_s + \bar{\nu}_\tau \rightarrow \nu_\tau + \bar{\nu}_\tau$	1	$4(p_1 \cdot p_4)(p_2 \cdot p_3)$
$\nu_s + \nu_\tau \rightarrow \nu_\tau + \nu_\tau$	1/2	$2(p_1 \cdot p_2)(p_3 \cdot p_4)$
$\nu_s + \bar{\nu}_\tau \rightarrow \nu_{e(\mu)} + \bar{\nu}_{e(\mu)}$	1	$(p_1 \cdot p_4)(p_2 \cdot p_3)$
$\nu_s + \bar{\nu}_{e(\mu)} \rightarrow \nu_\tau + \bar{\nu}_{e(\mu)}$	1	$(p_1 \cdot p_4)(p_2 \cdot p_3)$
$\nu_s + \nu_{e(\mu)} \rightarrow \nu_\tau + \nu_{e(\mu)}$	1	$(p_1 \cdot p_2)(p_3 \cdot p_4)$
$\nu_s + \bar{\nu}_\tau \rightarrow e^+ + e^-$	1	$4[(\tilde{g}_L^2(p_1 \cdot p_4)(p_2 \cdot p_3) + g_R^2(p_1 \cdot p_3)(p_2 \cdot p_4) + \tilde{g}_L g_R m_e^2(p_1 \cdot p_2))]$
$\nu_s + e^- \rightarrow \nu_\tau + e^-$	1	$4[\tilde{g}_L^2(p_1 \cdot p_2)(p_3 \cdot p_4) + g_R^2(p_1 \cdot p_4)(p_2 \cdot p_3) - \tilde{g}_L g_R m_e^2(p_1 \cdot p_3)]$
$\nu_s + e^+ \rightarrow \nu_\tau + e^+$	1	$4[g_R^2(p_1 \cdot p_2)(p_3 \cdot p_4) + \tilde{g}_L^2(p_1 \cdot p_4)(p_2 \cdot p_3) - \tilde{g}_L g_R m_e^2(p_1 \cdot p_3)]$

**Table 2:** Matrix elements for scattering processes;  $\tilde{g}_L = g_L - 1 = -\frac{1}{2} + \sin^2 \theta_W$  and  $g_R = \sin^2 \theta_W$ .



## References

- [1] KARMEN Collaboration, B. Armbruster *et al.*, Phys. Lett **B348** (1995) 19.
- [2] KARMEN Collaboration, K. Eitel *et al.*, Nucl. Phys. Proc. Suppl. **77** (1999) 212.
- [3] M. Daum *et al.*, Phys. Lett. **B 361** (1995) 179.
- [4] V. Barger, R.J.N. Phillips and S. Sarkar, Phys. Lett. **B 352** (1995) 365; **B356** (1995) 617(E).
- [5] J. Govaerts, J. Deutsch and P.M. Van Hove, Phys. Lett **B389** (1996) 700.
- [6] D.V. Ahluwalia and T. Goldman, Phys. Rev. **D56** (1997) 1698.
- [7] D. Choudhury and S. Sarkar, Phys. Lett. **B374** (1996) 87.
- [8] D. Choudhury, H. Dreiner, P. Richardson and S. Sarkar, hep-ph/9911365.
- [9] S.N. Gninenko and N.V. Krasnikov, Phys. Lett. **B434** (1998) 163.
- [10] R. Bilger *et al.*, Phys. Lett. **B446** (1999) 363.
- [11] S. Gninenko, private communication.
- [12] I. Goldman, R. Mohapatra and S. Nussinov, hep-ph/9912465.
- [13] M. Kachelrieß, hep-ph/0001160.
- [14] A.D. Dolgov, S.H. Hansen and D.V. Semikoz, Nucl. Phys. **B503** (1997) 426; Nucl. Phys. **B543** (1999) 269.
- [15] A.D. Dolgov, S.H. Hansen and D.V. Semikoz, Nucl. Phys. **B524** (1998) 621.
- [16] A.D. Dolgov, S.H. Hansen, S. Pastor and D.V. Semikoz, Nucl. Phys. **B548** (1999) 385.

- [17] R. Barbieri and A. Dolgov, Phys. Lett. B **237** (1990) 440; Nucl. Phys. **B349** (1991) 743.
- [18] K. Enqvist, K. Kainulainen and M. Thomson, Nucl. Phys. **B373** (1992) 498.
- [19] D. Nötzold and G. Raffelt, Nucl. Phys. **B307** (1988) 924.
- [20] K. Enqvist, K. Kainulainen and V. Semikoz, Nucl. Phys. **B374** (1992) 392.
- [21] L. Kawano, Fermilab-Pub-92/04-A (1992).
- [22] D. Tytler, J. M. O'Meara, N. Suzuki and D. Lubin, to appear in Physica Scripta, astro-ph/0001318.
- [23] G. Raffelt, Stars as Laboratories for Fundamental Physics (University of Chicago Press, Chicago, 1996).
- [24] G. Raffelt, Annu. Rev. Nucl. Part. Sci. **49** (1999) 163.
- [25] K. Kainulainen, J. Maalampi and J.T. Peltoniemi, Nucl. Phys. **B358** (1991) 435.
- [26] G. Raffelt and G. Sigl, Astropart. Phys. **1** (1993) 165.
- [27] W. Keil, H.-T. Janka and G. Raffelt, Phys. Rev. **D51** (1995) 6635.
- [28] A. Burrows, T. Ressel and M. Turner, Phys. Rev. **D42** (1990) 3297.

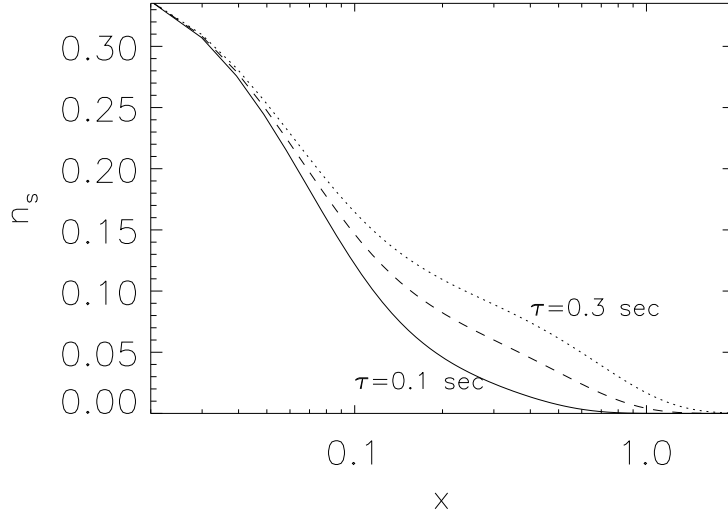


Figure 1: The normalized number density,  $x^3 n_{\nu_s}$ , as a function of  $x$  for the lifetimes 0.1 sec (solid), 0.2 sec (dashed) and 0.3 sec (dotted).

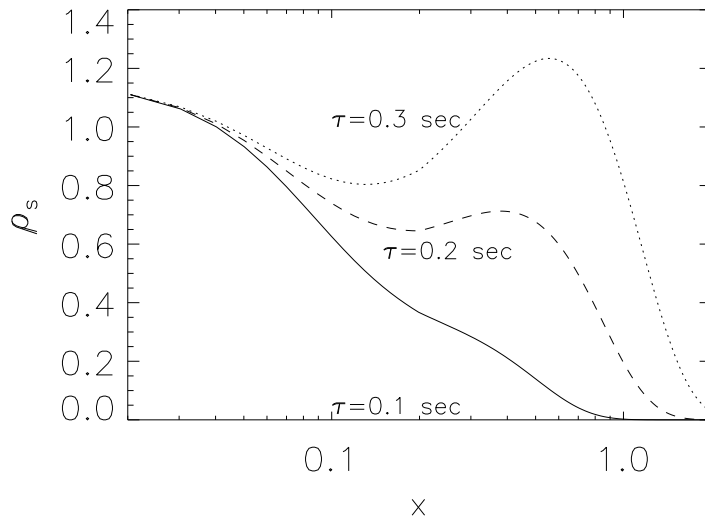


Figure 2: The normalized energy density,  $x^4 \rho_{\nu_s}$ , as a function of  $x$  for the lifetimes 0.1 sec (solid), 0.2 sec (dashed) and 0.3 sec (dotted).

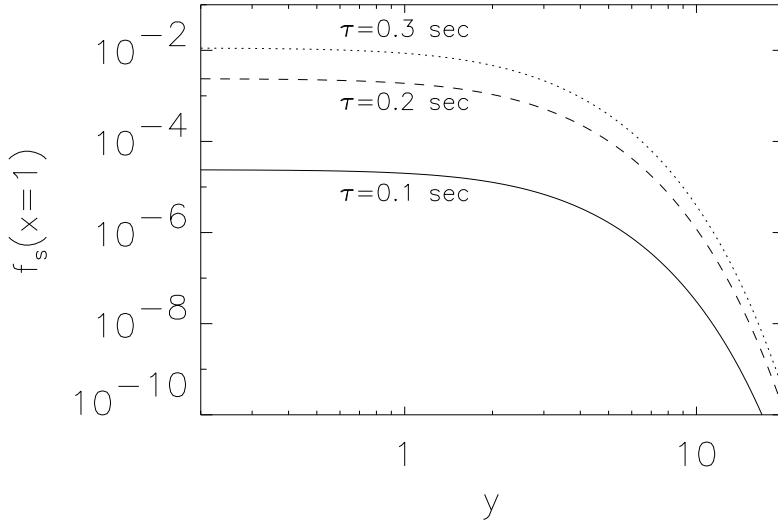


Figure 3: A snap-shot of the distribution function,  $f_{\nu_s}(y)$ , at the time  $x = 1$  for the lifetimes 0.1 sec (solid), 0.2 sec (dashed) and 0.3 sec (dotted).

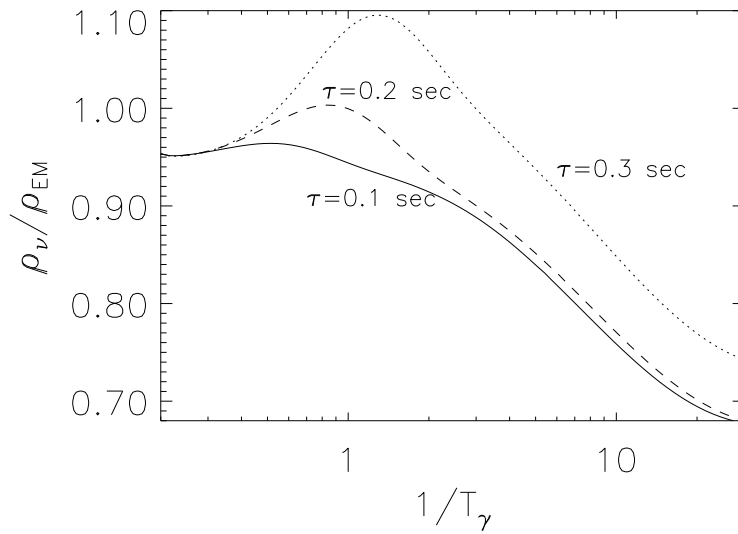


Figure 4: The energy density of all the active neutrinos divided by the energy density in the electromagnetic plasma,  $\sum \rho_{\nu} / \rho_{EM}$ , as a function of  $x$  for lifetimes 0.1 sec (solid), 0.2 sec (dashed) and 0.3 sec (dotted).

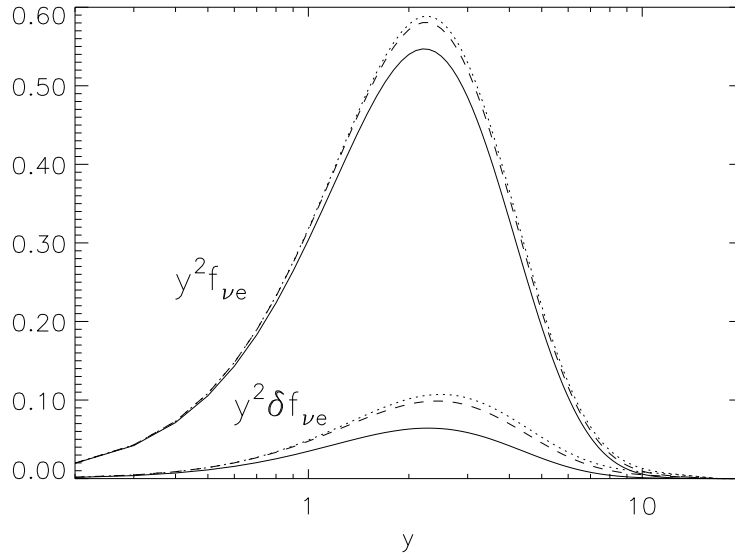


Figure 5: A snap-shot of the spectrum of  $\nu_e$ , namely  $y^2 f_{\nu_e}$  and the distortion  $y^2 \delta f_{\nu_e}$  at  $x = 1$ . The lifetimes are 0.1 sec (solid), 0.2 sec (dashed) and 0.3 sec (dotted).

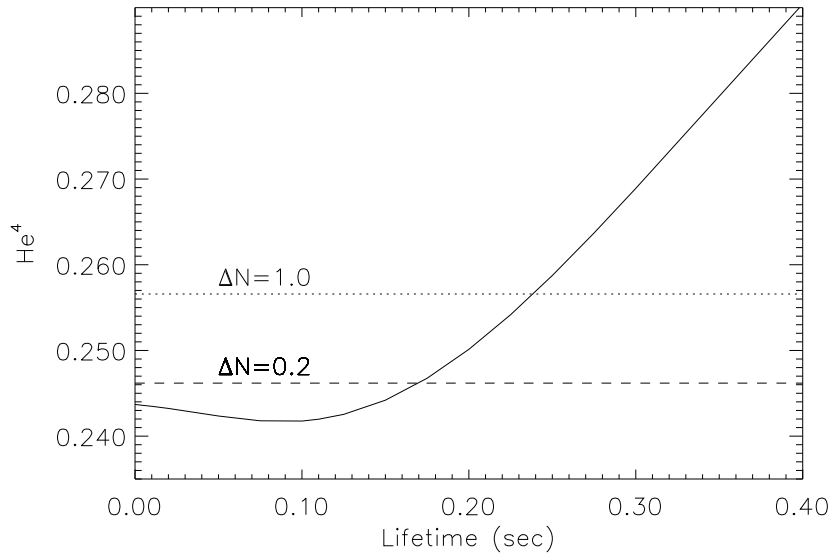


Figure 6: The final helium abundance as a function of lifetime. The horizontal lines correspond to  $\Delta N = 0.2$  and 1.0 extra effective neutrino species.

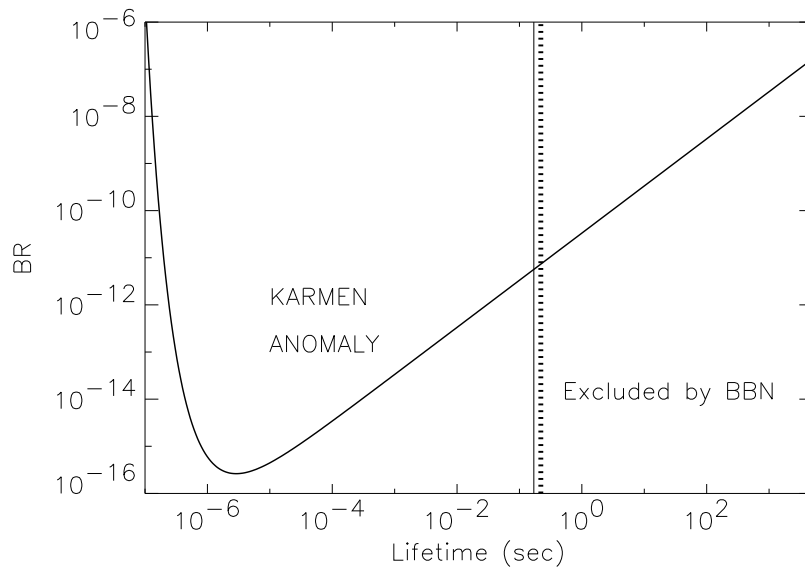


Figure 7: Branching ratio versus lifetime. A comparison of the KARMEN experimental data and the bound obtained here. The BBN bound excludes lifetimes bigger than 0.17 sec. The SN 1987A bound excludes the entire region presented.